Coupled CFD-FE-Analysis for the Exhaust Manifold of EF7 Engine

Conference Paper · January 2024

3 authors, including:

Aghil Askari
5 PUBLICATIONS **43** CITATIONS
SEE PROFILE

M. Farzin
Isfahan University of Technology
62 PUBLICATIONS **674** CITATIONS
SEE PROFILE

Coupled CFD-FE-Analysis for the Exhaust Manifold of EF7 Engine

A. Askari, M. Farzin and E. Shirani

Department of Mechanic Engineering

Isfahan University of Technology, Isfahan 84156-83111, Iran

e-mail: aghilaskari@yahoo.com

e-mail: m.farzin@cc.iut.ac.ir

e-mail: e.shirani@cc.iut.ac.ir

Abstract. *Stainless steels are now widely used for automotive exhaust systems, driven by the need to increase the durability of exhaust systems, which are subjected to severe conditions and include components of high technology such as manifold, catalytic converter and particle filter. This causes a direct consequence of the effort to decrease automotive pollutant emissions due to the new environmental regulations throughout the world. During the last few years, the increasing use of stainless steel fabricated exhaust systems has led us to study new production technologies of forming and welding. Modern exhaust systems must withstand severe cyclic mechanical and thermal loads in an engine cycle. Up to now, highly loaded parts of exhaust systems are predominantly designed experimentally by means of lengthy and expensive component tests. A further shortening of development time without quality loss is possible only by increasing application of computer simulation. The aim of a series of coupled computational fluid dynamics-finite element, CFD-FE, simulations performed here, was to investigate the thermo-mechanical behavior of a stainless steel engine exhaust manifold which is in early stage of design. It is going to be designed for the national diesel engine of IPCO, EF7, instead of the existing cast iron one. For this purpose, both fluid flow and solid walls are considered simultaneously. We assume that there is steady state, incompressible and turbulent flow with k-ε turbulence model. Since the failure of the exhaust manifold is mainly due to the geometric constraints of the less expanded inlet flange and cylinder head, the analysis is based on exhaust system model with three-dimensional temperature distribution and temperature dependent material properties. Large compressive plastic deformations are observed for the elevated temperature of thermal shock cycles.*

Key words: CFD-FE Coupling, Heat Transfer, Thermal Stress, Exhaust Manifold, Engine

1 INTRODUCTION

Exhaust manifolds are generally simple cast iron or stainless steel units, which collect engine exhaust from multiple cylinders and deliver it to the exhaust pipe. In order to decrease the pollutant emission and fuel consumption of vehicles, exhaust systems are becoming more and more developed, often including advanced technical components such as very thin-walled and low-weight exhaust manifolds. Thus to increase the durability and thermo mechanical fatigue, TMF resistance, exhaust manifolds are now widely made up of stainless steel bent tubes or stamped shells steel (rather than cast iron) from grades with very high temperature properties as well as forming ability [1,2].

An exhaust manifold is generally subjected to many repeated run-stop cyclic loadings. Most of the cracks found in the stainless steel exhaust manifold are caused by out-of-phase (OP) TMF, where the compressive strain occurs at high temperature. Although creep may have occurred at an elevated temperature, its effect on the fatigue life is relatively small because of the compressive state of strain. Therefore, the fatigue failure is dominated mainly by mechanical fatigue and plastic strain [3, 4].

Highly loaded parts of the engine systems are predominantly designed experimentally by means of lengthy and expensive component tests. To decrease the development cost and time, computer simulation should be utilized which at the same time, provides handling of the growing number of model variants and design optimization. This way, experiment is only needed at the end to verify the simulation results [5, 6].

The aim of a series of coupled computational fluid dynamics-finite element, CFD-FE, simulations performed here, was to investigate the thermo-mechanical behavior of a stainless steel engine exhaust manifold which is in early stage of design (fig 1). It is going to be designed for the national diesel engine of IPCO, EF7, instead of the existing cast iron one [7].

Fig 1. Under construction exhaust manifold sample.

2 Analysis Procedure

Typical thermo mechanical loading subjected to an exhaust manifold during car lifetime is very hard to define and is certainly not reproducible. Thus a standard durability simulation which corresponds to severe running conditions is typically performed. Figure 2 is the simple thermal shock mode used to simulate the thermal load cycle consisted by the heating and cooling process. One cycle consists of idling, full load at the rated speed that gives the maximum power and cooling process to ambient temperature [4, 7].

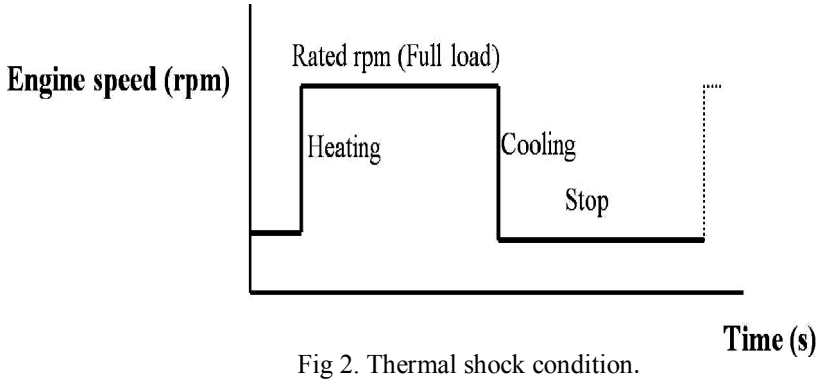

Fig 2. Thermal shock condition.

The process of the coupled CFD-FE analysis of the exhaust manifold is as following (fig 3):

1- Construction of the finite element model for the hot end exhaust system , simple cylinder head, bolts, gusset and the catalyst;
2- Construction of the CFD model for the runners from the cylinder head flange on the basis of FE model;
3- CFD analysis of exhaust manifold flow;
4- Mapping the heat transfer coefficients obtained from CFD analysis into the FE model;
5- Determining the temperature distribution during the thermal shock loading based on the input data from gas flow simulation;
6- Simulation of thermal behavior based on the thermal stress analysis which considers elasto-plastic material with temperature dependent properties using three - dimensional temperature data.
7- Optimization of the design to reduce plastic strain;

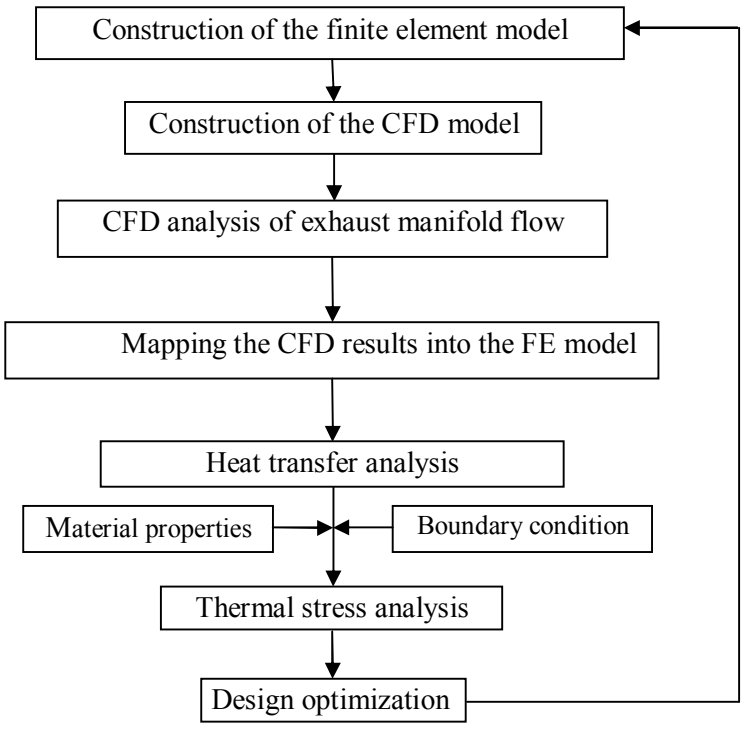

Fig 3. Analysis procedure of the exhaust manifold.

3 CFD Analysis

In the interest of good performance of the turbo charged engine a low pressure drop of the exhaust manifold is necessary. It is necessary to calculate the heat transfer coefficients as boundary conditions for the FE analysis. Therefore, the fluid flow and the heat transfer through the exhaust manifold are computed by a CFD analysis using the CFD code FLUENT. This procedure assumes a constant mass flow rate through all manifold gas admissions, so that always steady state conditions are calculated [15, 18].

CFD results are mapped subsequently on the ABAQUS-FE-mesh and used to obtain corresponding thermal deformations and stresses. This mapping operation is done by a code which is developed using MATLAB software.

3.1 Technical Approach

3.1.1 Geometry

To calculate the flow field in the exhaust manifold, the model should contain the runners from the cylinder head flange, the junctions and the surfaces up to the flange upstream the exhaust turbine (fig 4).

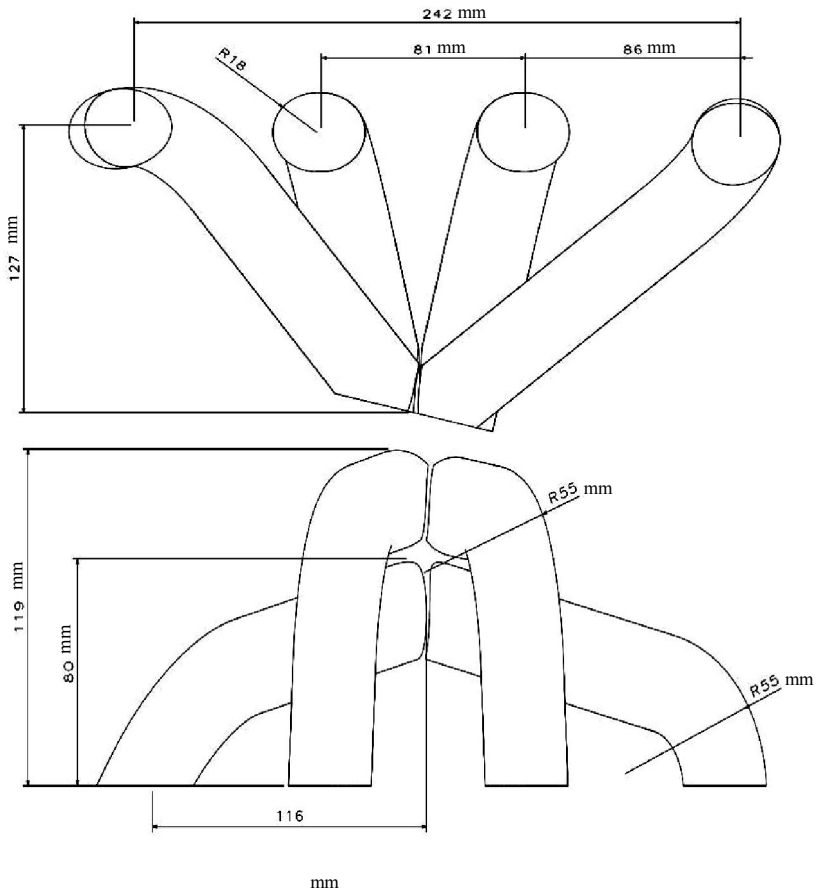

Fig 4. Computational domain

3.1.2 Mesh

For the CFD calculation a hybrid mesh with three sub layers consisting of 300.000 cells has been created (fig 5). In order to transfer the data accurately from the CFD code to the FE code, CFD mesh is constructed on the basis of the Fe elements of the manifold gas carrying surfaces [15, 18].

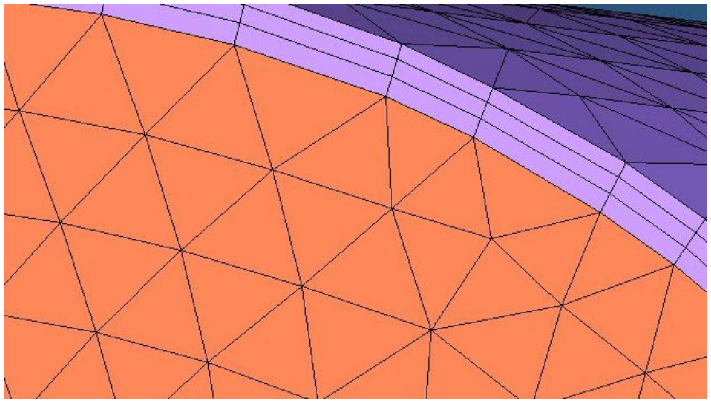

Fig 5. Unstructured mesh

3.1.3 Boundary conditions

The boundary conditions for the 3D CFD model are taken from the gas exchange 1D simulation with GT Power software when engine operates with full load with 6000 rpm (figure 6). With this software it is possible to get the flow conditions at every point of the model. Data of mass flow rate, temperature and pressure have been taken as boundaries conditions for the CFD model. For the steady state calculations the point with the maximum mass flow is most interesting. At this point the exhaust blow causes the maximum pressure drop [18].

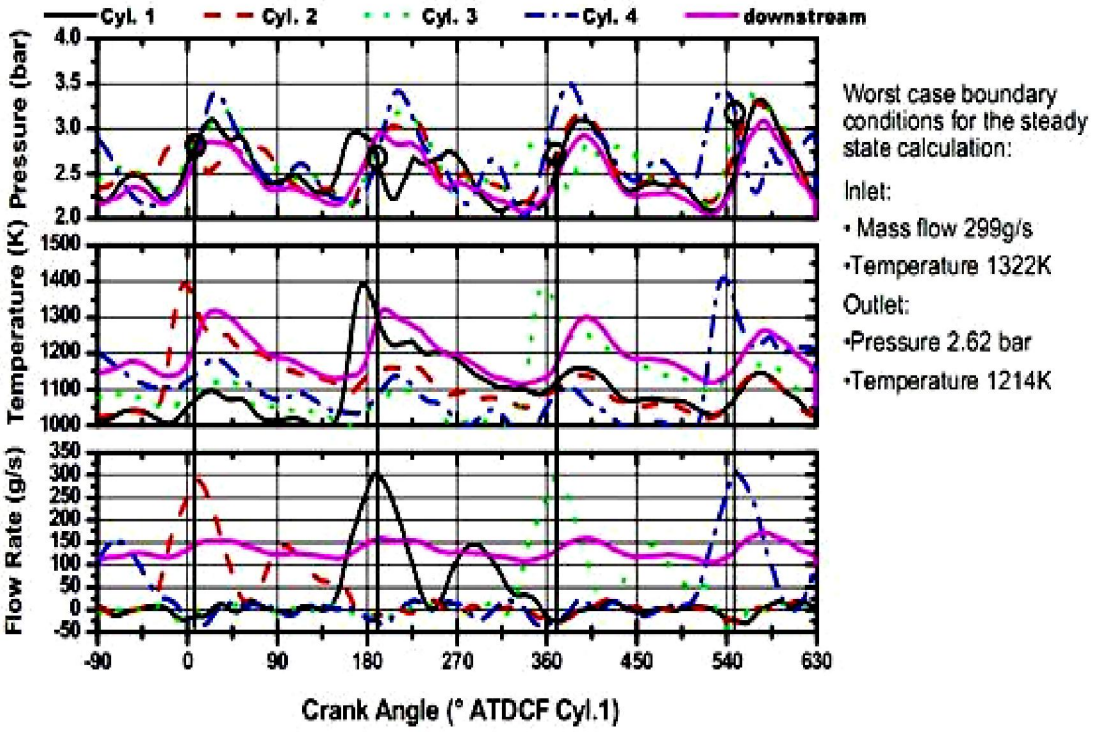

Fig 6. Boundary conditions for CFD calculation.

3.1.4 Flow specification and assumptions for the FLUENT calculation

The Flow specification and assumptions for steady state CFD calculations is:

- Turbulent flow with k-ε turbulence model is considered.
- Mass flow inlet and pressure outlet are specified as boundary conditions.
- Flow is considered incompressible and the gas is assumed perfect gas.
- The differencing scheme for exhaust system calculation is upwind, a first order scheme.
- The method for pressure and velocity coupling is SIMPLE for the steady state CFD calculations.

During the time of one working cycle when the engine operates with 6000 rpm at full load, the variation in exhaust gas temperature will only slightly influence the wall temperature distribution due to the short time nature and small geometry. In contrast to this, the variation in velocity has a large effect on the heat transfer into the manifold wall through the heat transfer coefficient. The higher the local velocity, the higher the Reynolds number and therefore via the Nusselt number the higher the heat transfer coefficient. This is the reason why wall boundary is set to the fixed temperature of 875°C but CFD analysis is done to obtain heat transfer coefficients [4, 18].

3.2 CFD results

Figure 7 shows the Mach numbers at the exhaust manifold surfaces. The Mach numbers are low, M < 0.3, for all cylinders. The bends are smooth enough and thus the flow acceleration at these bends is moderate.

Figure 8 shows the total pressure at the exhaust manifold surfaces. All cylinders have similar total pressure level at outlet section. The pressure level for the cylinders 1 or 4 is a little bit higher than the others because the geometry has an additional bend.

Figure 9 shows the heat transfer coefficients (HTC) at the inner wall of the exhaust manifold. The highest values are in the runners inlet region where the gas flow has the highest velocity. Also, at these regions, turbulent flow causes the high values of HTC. The highest value (282 W/m2K) is not in the critical level.

Table 1 includes the total pressure drop from the cylinder head flange to the turbine flange for each cylinder. The pressure drop for the cylinders 1 or 4 is a little bit higher than the others because the changing of the flow direction is not as smooth as the flow in the other cylinders and also the distance between the two bends is shorter.

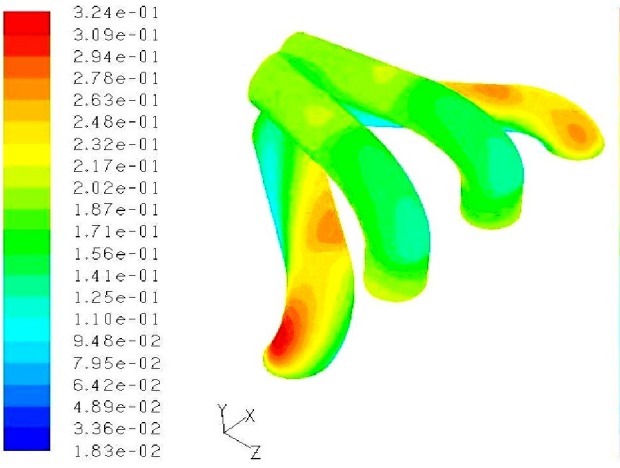

Fig 7. Mach number at the exhaust manifold surface.

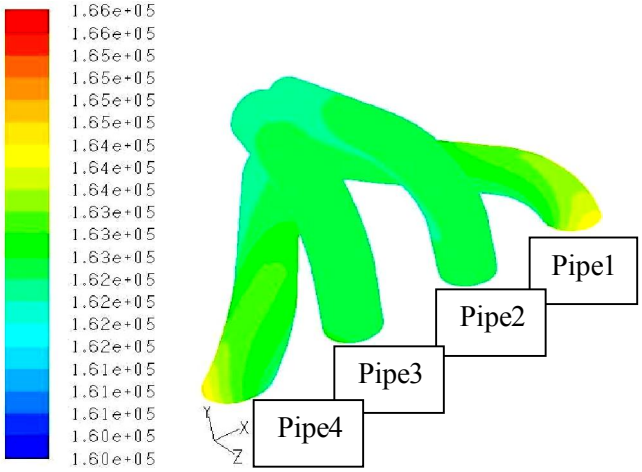

Fig 8. Total absolute pressure distribution.

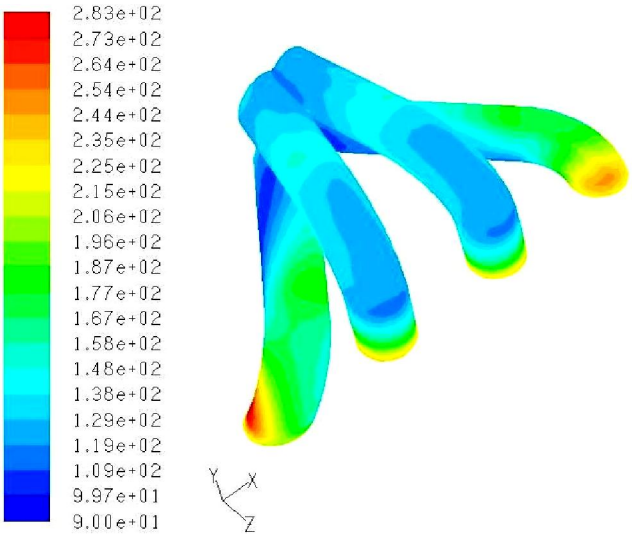

Fig 9. Heat transfer coefficient @6000rpm.

Table 1. Total pressure loss

	Total Pressure Loss Flange to Flange (mbar)
Cylinder 1	190
Cylinder 2	110
Cylinder 3	103
Cylinder 4	220

3.3 Optimization Criteria

To optimize the flow behavior in an exhaust manifold the following criteria must be held:

- No high total pressure,
- No high Mach number,
- Low and similar pressure drop in all cylinders.

These conditions can be achieved by optimizing exhaust manifold design. The modifications include the complete design upstream and downstream the catalyst. The parameters for an optimization are:

- Pipe diameter.
- Pipe bends.
- The shape of the pipe junctions.
- The shape of flange between the turbine and the pipe [7, 16].

4 FE Analysis

To simulate the thermally induced stresses and deformations induced by the temperature distributions FE simulations have been performed using ABAQUS (Version 6.8). The thermo mechanical load is a result of material expansion due to the high temperatures.

In this investigation the value and the distribution of the plastic strain at the end of second cycle have been considered as an indicator for the possible structural failure [7, 17].

4.1 Technical Approach

Generally the FEM calculations can be divided into the parts “Thermal Analysis” (calculation of the temperature distribution at engine operation) and “Structural Analysis” (simulation of load history and assessment of durability) [2, 7].

The thermal analysis is executed in a pre-step in order to calculate the temperature distribution of the engine for operation at rated power. The resulting nodal temperatures are an additional boundary condition in the subsequent structural analysis.

The results of thermo mechanical analysis act very sensitive versus temperature distribution. Additionally the material behavior has to be temperature depended and exactly defined at low and high temperature.

The thermal boundary conditions are divided into internal and external surface. The boundary condition of internal surface comes from the forced convection with the exhaust gas. The estimation of local convection coefficients needs a fair knowledge of both the fluid

flow near the manifold wall and the gas temperature. The resolution of this fluid problem is performed using the commercial FLUENT code. This commercial code and the method to calculate the heat transfer coefficient were described before.

With help of a code developed in MATLAB, the HTC's will be mapped on the FE mesh for the thermo mechanical analysis. Fig 10 shows the results of CFD-Analysis and the mapped values on FE mesh for the structure analysis.

For the external surface of exhaust manifold the correct HTC'S to define is difficult. Due to the high temperature of pipes, the heat exchange on the external surface has to be modeled using both natural convection with air at room temperature and radiation. The boundary conditions on the outside of the component were only roughly adjusted so that the model temperatures match the measured ones at specific locations of the manifold surface. This confirms again that the inner heat transfer mainly influences the temperature behavior of this component.

4.2 Finite element model

Fig 11 shows the finite element model for the heat transfer and thermal stress analysis. It is composed of the exhaust manifold, simple cylinder head, bolts, conical bush and the catalyst. Though the manifold is made up of 1.5 mm thick bent tubes, we constructed it with two layered 8 node brick elements because the temperature difference between the outside and inside of the tubes imposes a high gradient through the thickness. The conical bush is modeled with second order tetrahedron elements and the catalyst is modeled with shell elements and the cylinder head, bolts and the gusset are also modeled with brick elements [2, 13].

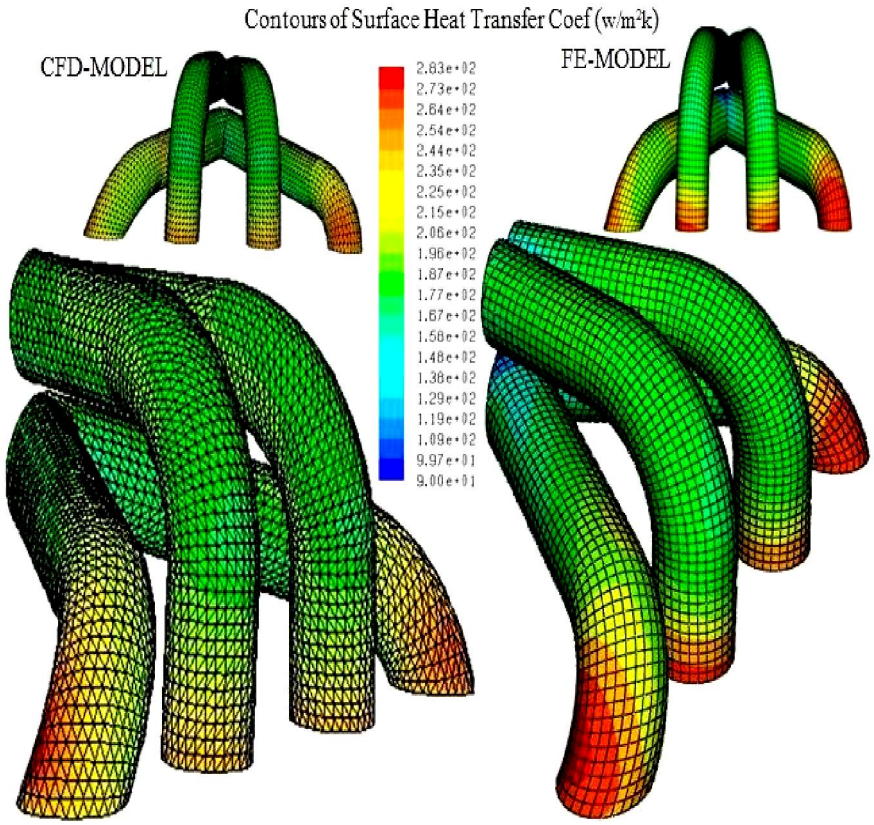

Fig 10. Mapping the CFD results on the Fe model.

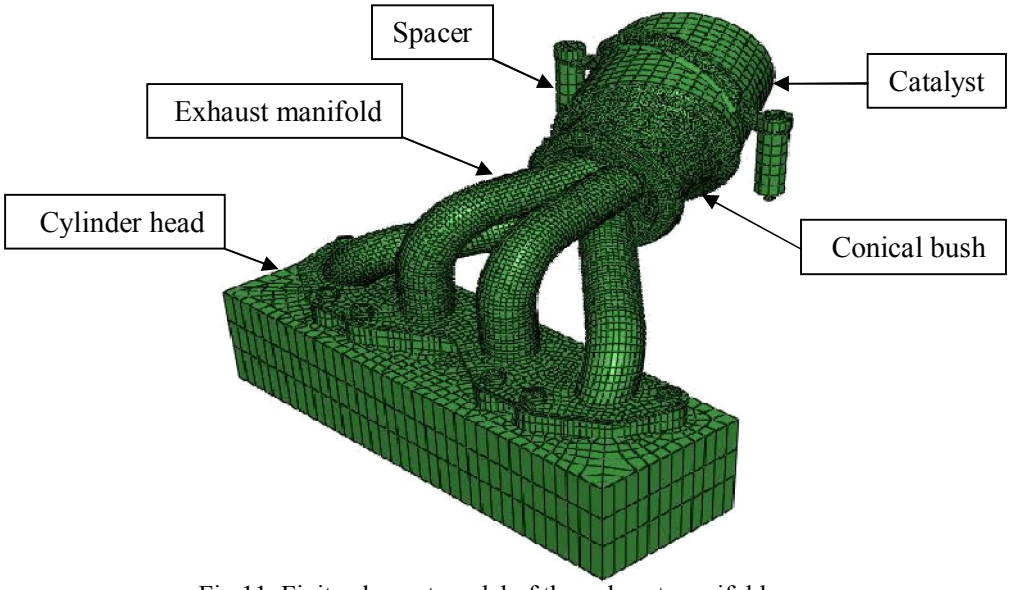

Fig 11. Finite element model of the exhaust manifold.

4.3 Input data for the FEA calculations

Inputs for the FEA are divided into thermal and mechanical boundary conditions and loads.

4.3.1 Thermal boundary conditions and loads

Thermal cyclic loading is applied as 3-D temperature distribution to the finite element model. It is composed of two steps; heat up and cool down. During the heat up process, the entire model is heated from room temperature to the maximum temperature distribution obtained from the CFD analysis. And, during the cool down process, the assembly model goes back to room temperature in a steady state condition. Figure 12 shows the load steps with prescribed load history of one cycle [4].

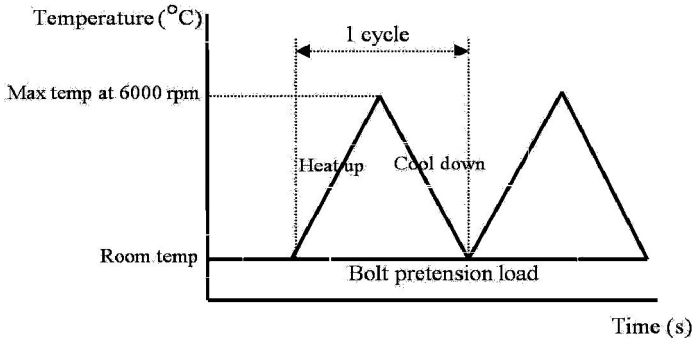

Fig 12. Load step during thermal shock test.

The thermal boundary conditions are heat transfer coefficient and the gas/environment temperature of internal and external surfaces of manifold. The heat transfer coefficients for the internal surface are coming from CFD Analysis, the gas temperature (= 875°C) from Gas Exchange Analysis. The environment temperature is assumed as 35°C. The determination of heat transfer coefficient at the external surface of manifold is already described in 4.1 and is $\alpha_{external}$ = 30 W/mK.

4.3.2 Mechanical boundary conditions and loads

Beside the thermally induced strains, the exhaust gas manifold is subjected to mechanical loadings due to the fixing screws and the differential gas pressure on the inner surfaces. Under normal conditions, the influence of the pressure differences can be neglected for this kind of solid component, because the pressure of the cooling flow and the exhaust flow in the exhaust manifold vary between 2.0 and 3.0 bar depending on the operating point. The stresses induced by these pressures are relatively low in comparison to the thermal stresses induced by the temperature distribution. Therefore they are considered to be negligible within the scope of this investigation.

Only the fixing screws may introduce a considerable mechanical load [14, 15]. For all the clamping bolts at the cylinder head flange the pre-load is assumed as 16.5 KN according to IPCO experience.

To assure correct boundary conditions on the side of the cylinder head, the gasket between these two components and its non-linear compressive behavior has been modeled as well. The connection between manifold and conical bush is realized with a clamp strip. This contact will be considered for the calculation as a stiff connection and means no relative movement between manifold and bush. The catalyst is welded to conical bush also the bracket and catalyst are welded together i.e. no relative movement [7].

4.4 Material properties

In the design process the austenitic stainless steel type 304 is decided for the material of the manifold. St304 is a family of alloys with sufficient nickel to produce an austenitic structure which has unique and superior properties. It is heat resistance and has excellent resistance to growth and oxidation at temperature up to 1050°C. Low coefficient of thermal expansion with good thermal shock resistance is a typical property of this material and used in gas turbines, turbocharger housing, exhaust manifold and hot pressing dies [12]. The widespread use of austenitic stainless steels in elevated temperature conditions indicates their attractive thermo-mechanical properties [10, 11].

Fig 13 shows the stress-strain relationship at different temperatures and the mechanical and thermo-physical properties of Stainless steel 304 are shown in Table 2.

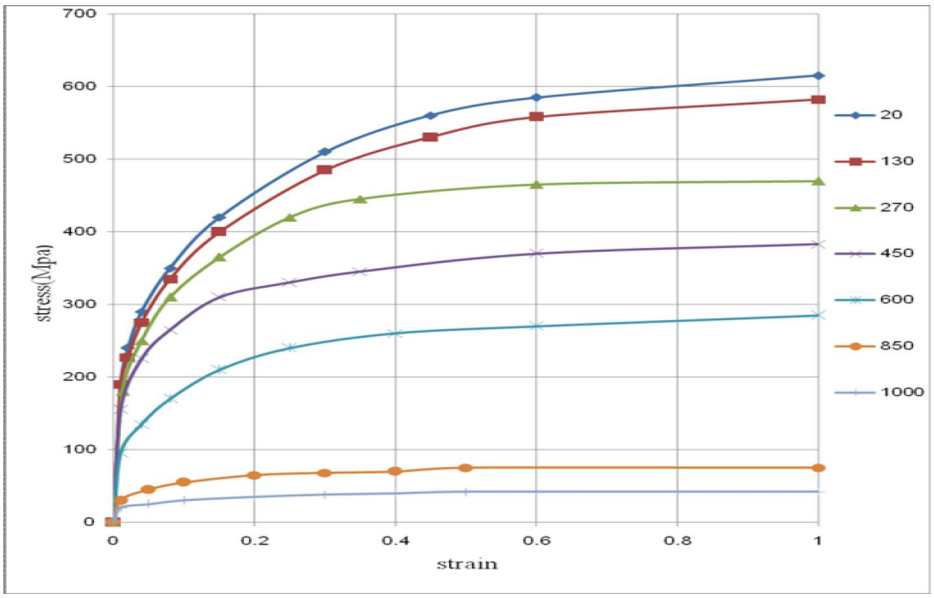

Fig 13. Stress-strain behavior of stainless steel 304 at different temperatures [12].

Table 2. Material properties of stainless steel 304[12].

Temperature (°C)	Modulus of Elasticity (GPa)	Thermal Conduction (J/mm °C s)	Thermal Expansion ($°C^{-1}$)	Poison' ratio
0	198.50	0.0146	$1.70e^{-5}$	.294
100	193.00	0.0151	$1.74.e^{-5}$	.295
200	185.00	0.0161	$1.80e^{-5}$	.301
300	176.00	0.0179	$1.86e^{-5}$	.310
400	167.00	0.0180	$1.91e^{-5}$	.318
600	159.00	0.0208	$1.96e^{-5}$	.326
800	151.00	0.0239	$2.02e^{-5}$	.333
1200	60.00	0.0322	2.07e-5	.339

4.5 Heat Transfer Analysis

The objective of the heat transfer analysis is to capture the three-dimensional temperature distribution of the exhaust system. This is a dominant step of the coupled CFD-FE analysis, because the accuracy of thermal data governs the accuracy of the mechanical response of the structure [4, 19].

The input data are gas temperature and the internal heat exchange coefficient which come from gas flow simulation in the exhaust pipes in steady state, incompressible, and turbulent model [7]. The temperature field is then calculated in a steady-state condition in a finite element code and Fig 14 shows the temperature field at the end of heating. The maximum temperature uniformly occurs in the manifold tubes, where the high temperature gas flows in a short thin-walled passage very fast.

In compare to the rest of manifold the flange has relative low temperature value. It results from two reasons; (i) exhaust gas doesn't contact with the flange, and (ii) heat is transferred from inlet flange to the cylinder head, because the cylinder head has lower temperature compared to the exhaust manifold due to the coolant. Therefore the thermal expansion of manifold is much higher as flange's thermal expansion and because of that the expansion of manifold will be impeded with flange [4].

4.6 Thermo-mechanical stress analysis

In order to perform the elasto-plastic thermal stress analysis, it is necessary to consider the temperature distribution, mechanical constraints, and temperature dependent material properties. The main element of the loading is the thermal load and the only mechanical load is the bolt tightening which can be represented rather easily. The bottom surface of the simple cylinder head and the vertical supporting bolts of the catalyst are constrained.

The analysis is carried out in three steps for the same model of the thermal analysis; first, bolt pretension load is applied, and then the heat up and cool down processes of the thermal shock happen respectively. The heat up and cool down processes will be repeated for one another time [2,4,7].

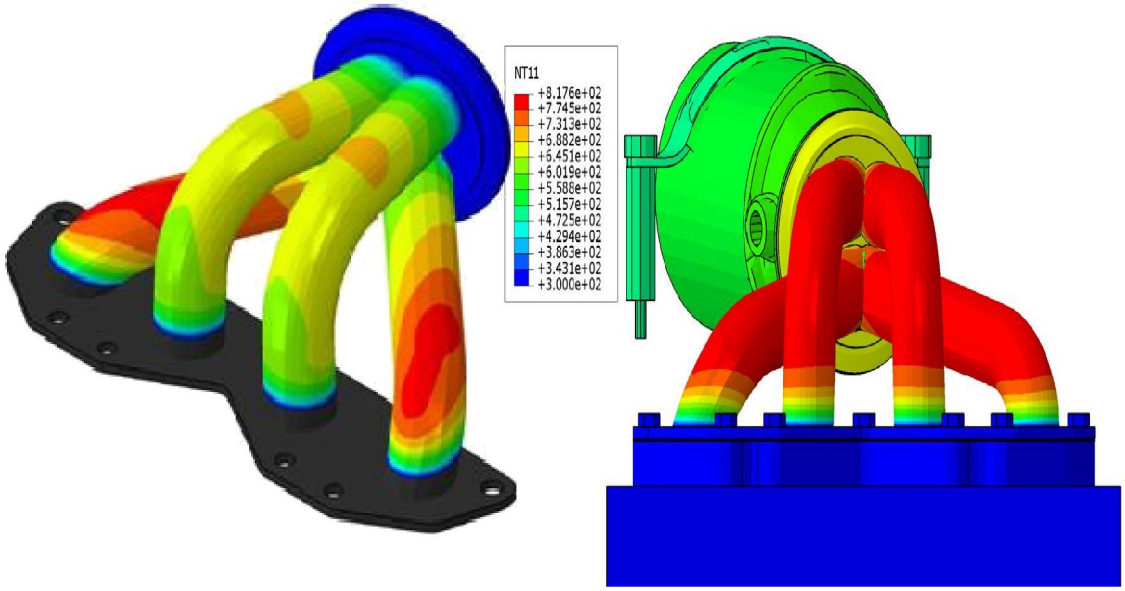

Fig 14. Temperature field at the end of heating.

4.7 Results of the FEM simulation

Realizing the fact that crack initiation and crack propagation in ductile materials is preceded by the development of localized plastic deformation zones the values as well as the distribution of this scalar strain is the best indicator for possible structural regions failure. With this critical regions of the structure may be detected clearly and non-ambiguous. This will be considered as an indicator for the possible structural failure. But it is difficult to find the acceptable limit for the plastic strain. According to IPCO experience the maximum plastic strain at the end of second cycle is to hold less as 1% [7].

The distribution of plastic strain at the end of second cycle is determinate (fig 15). There are some areas with plastic strain more as 1%. the maximum value is 2.8%. In this calculation all the cylinder head bolts at flange are fix and relative movement of flange at the gasket's plan is not possible.

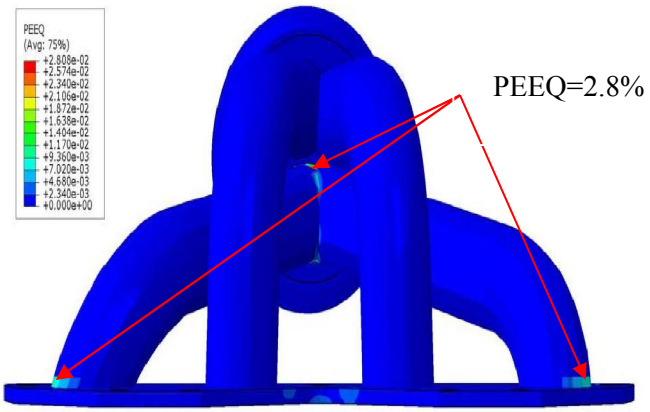

Fig 15. Equivalent plastic strain range at situation of no relative movement of flange.

For the assembly of manifold one bolt must be used as fixing point i.e. there is small tolerance between bolt's shaft with 8mm diameter and the bore with 8.5 mm diameter. Other bolts might have a bigger diameter as the bolt's shaft. This makes the relative movement of flange possible.

With this boundary condition the distribution of plastic strain at the end of second cycle is

determinate and shown in fig 16 The expansion of flange is now not stopped and can slide at the gasket's plan. As the result there is no area with high plastic strain in the manifold to observe. Fig 17 shows the maximum movement of bores relative to fix bolt at the gasket's plan in both directions. This movement is necessary to get no high plastic deformation in manifold. To make the machining easier, can the bores drilled with constant diameter 10.5 mm.

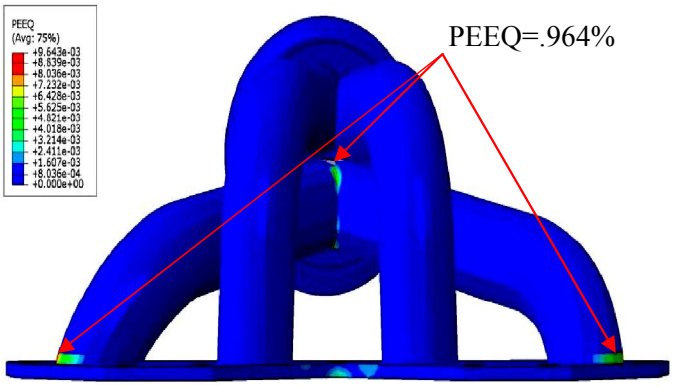

Fig 16. Equivalent plastic strain range at situation of relative movement of flange.

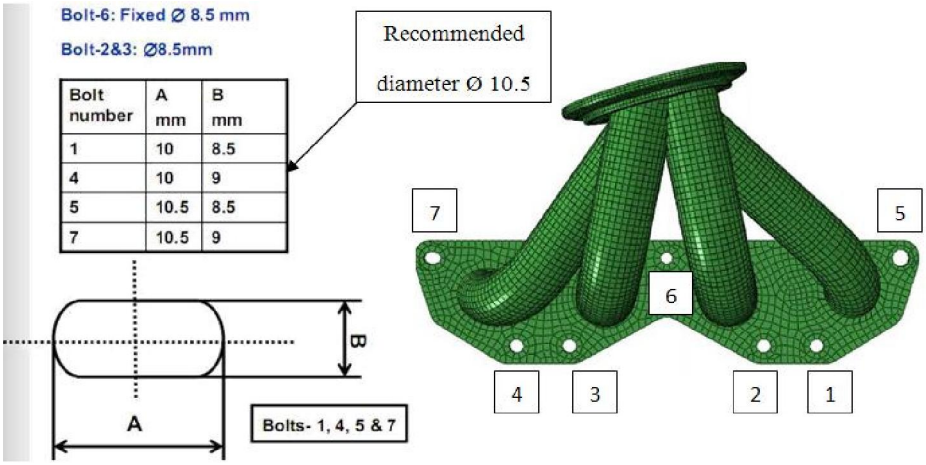

Fig 17. Max bores movement at gasket' plane relative to fixed bolt.

5 Discussion / Conclusions

The modeling with the elements of type C3D8I, the use of at least two elements across the wall thickness of the exhaust manifold and the nonlinear analysis enable a reasonable simulation of a rather complex problem and ensure relatively realistic predictions of the thermal gradients occurring under extreme conditions. It can be seen that plastic strain which has the dominated effect on the damage evolution, is maximum at the junctions where the expansion of the tubes is restricted by flanges and the cylinder head. The results of this investigation confirm that significant plastic strain can be expected at selected areas of the component. The equivalent plastic strain concentrations can be interpreted as remarkable indices for extreme level of temperatures and temperature gradients and as an indicator for the possible structural failure and show at the same time the sensitive areas for potential enhancement measures. Next development steps of the exhaust manifold will be taken based on these informations.

6 References

[1] W. Schmitt, R. Mohrmann, H. Riedel, A. Dietsche and A. Fischersworring-Bunk, "Modelling of the Fatigue Life of Automobile Exhaust Components", in: Proceedings of Fatigue 2002, Stockholm, June 2002, to appear.

[2] S. Yoon, K.O. Lee, S.B. Lee and K.H. Park, "Thermal Stress and Fatigue Analysis of Exhaust Manifold", Key Eng. Mat. Vol. 261-263 (2004), pp. 1203-1208.

[3] Y. WATANABE et Al. "Thermal Fatigue Life Prediction for Stainless Steel Exhaust Manifold", SAE Technical paper series 980841, ASTM STP 520 (1998), pp. 147-152.

[4] B. L. Choi, H. Chang and K. H. Park, "Low cycle thermal fatigue of the engine exhaust manifold", Int. Journal of Automotive Technology, Vol. 5 (4) (2004), pp. 297-302. [5] Gary. R. Halford, "Low-cycle thermal fatigue", Lewis Research Center, 1986.

[6] Riedler M., Leitner H., Prillhofer B., Winter G., Eichlseder W. "Lifetime simulation of thermo-mechanically loaded components", Meccanica 42 (1) (2007), pp. 47–59.

[7] Dr.-Ing. F. Haubner, Dipl.-Ing. N. Moshiri."Stress and Thermal Analysis of exhaust manifold NA IPCO EF7 Engine" FEV CAE report of EF7 exhaust manifold, 2005

[8] J. Jian Ping and S. Yi, "A continuum damage mechanics model on low cycle fatigue life assessment of steam turbine rotor", Int. J Pressure Vessels Piping 78 (1) (2001), pp. 59–64.

[9] Jing J.-P., Meng G., "On the fatigue-creep damage analysis of a steam turbine rotor by a nonlinear continuum damage mechanics model", Zhongguo Dianji Gongcheng Xuebao/Proceedings of the Chinese Society of Electrical Engineering, 23 (9) (2003), pp. 167-172.

[10] SEKITA Takashi, "Materials and Technologies for Automotive Use", JFE TECHNICAL REPORT No. 2 (Mar. 2004)

[11] F. Placidi, S. Fraschetti. "Potential application of stainless steel for automobile crash worthiness structures", Centro Sviluppo Materiali S.p.A Italy

[12] D. Deng, H. Murakawa. "Numerical simulation of temperature field and residual stress in multi-pass welds in stainless steel pipe and comparison with experimental measurements" Int. J. of Computational Materials Science, (2005), Article in press.

[13] ABAQUS User's Manual, Version 6.8.

[14] K.Hoschler,J.Bischof,W.Koschel,''Thermo mechanical Analysis of an Automotive Diesel Engine Exhaust Manifold,' Elsevire science Ltd. and ESIS,2002.

[15] Y. Degar, B. Simperl, L. P. Jimenez. "Coupled CFD-FE-Analysis for the Exhausted Manifold of a Diesel Engine", ABAQUS Users Conference, 2004.

[16] Constantine D.Rakopoulos, Evangelos G.Giakoumis., Diesel Engine Transient Operation, Springer-Verlag. 2009.Report, 2004 PP 78-132

[17] T.L.Anderson, Fracture Mechanics Fundamentals

[18] Dr.-Ing. F. Haubner, Dipl.-Ing. Oliver Rudwinsky. "CFD-Simulation Exhaust System IPCO EF7 engine" FEV CFD report of EF7 exhaust manifold ,2005.

[19] J.J. Thomas, L. Verger, A. Bignonnet and E. Charkaluk, "Thermomechanical design in the automotive industry", Fatigue Fract Eng Mater Struct 27 (2004) (10), pp. 887–895.

[20] A.M.P. de Jesus, A.S. Ribeiro and A.A. Fernandes, "Finite Element Modeling of Fatigue Damage Using a Continuum Damage Mechanics Approach", J. of Pressure Vessel Technology, Vol. 127 (2005).

[21] N. Bonora, G. M. Newaz, "Low cycle fatigue life estimation for ductile metals using a nonlinear continuum", Int. J. Solids Structures Vol. 35 (16) (1998), pp. 1881-1894.